Preprints.org

Article

Cell Recruitment and the Origin of Anterior-Posterior Asymmetry in the *Drosophila* Wing

Rosalio Reyes , Rafael Rodriguez-Muñoz , Marcos Nahmad [*]

Article

Cell Recruitment and the Origin of Anterior-Posterior Asymmetry in the *Drosophila* Wing

Rosalío Reyes [1,2], Rafael Rodríguez-Muñoz [1] and Marcos Nahmad [1,*]

[1]   Department of Physiology, Biophysics, and Neurosciences; Center for Research and Advanced Studies of the National Polytechnic Institute (Cinvestav-IPN); Mexico City, 07360; MEXICO

[2]   Present Address: Interdisciplinary Polytechnic Unit of Biotechnology of the National Polytechnic Institute; Mexico City, 07340; MEXICO

[*]   Correspondence: mnahmad@fisio.cinvestav.mx

Abstract: The mechanisms underlying the establishment of asymmetric structures during development remain elusive. The wing of *Drosophila* is asymmetric along the Anterior-Posterior (AP) axis, despite that its growth signals that drive its growth are presumably symmetric. Here, we investigated the contribution of cell recruitment, a process that drives wing fate differentiation in the *Drosophila*, to the asymmetric shape and pattern of the adult wing. Genetic impairment of cell recruitment results in a significant reduction in adult wing asymmetry primarily affecting the region between longitudinal vein 5 and the wing margin (L5-M). Morphometric analysis reveals that the lack of cell recruitment results in a more symmetric wing with respect to the AP, suggesting a contribution of cell recruitment to the establishment of asymmetry in the adult wing. A close examination of the expression of the wing selector gene *vestigial (vg)* in wing disc does not support this hypothesis. However, the circularity of the Vg pattern significantly increase in recruitment-impaired wing disc, suggesting that while the decrease of the L5-M region in the adult wing may not be attributed to cell recruitment, it could contribute to the overall asymmetry of the adult wing. We conclude that cell recruitment, a widespread mechanism that participates in growth and patterning of several developing systems, could drive, at least partially, the asymmetric shape of the *Drosophila* wing.

Keywords: Drosophila-wing; Anterior-Posterior; cell-recruitment; asymmetry; morphometrics

---

1. Introduction

The developmental origins of complex asymmetric structures are largely unclear. Since organ shape is closely related to function, there is considerable interest in understanding the developmental processes that guide the robust establishment of these asymmetric structures (Baker et al. 2008; Ferreira and Vermot 2017; Gormley and Nascone-Yoder 2003; Grimes and Burdine 2017; Le Garrec et al. 2017). One of the most studied mechanisms in bilateral organisms are the signaling pathways responsible for left-right asymmetries during the early stages of development (Bessodes et al. 2012; Little and Norris 2021; Smith and Uribe 2021). However, little is known about the establishment of asymmetric patterns and shapes using morphogenetic signals that diffuse symmetrically away from their source. The wing of *Drosophila melanogaster* is a biological system where the mechanisms of growth and patterning have been extensively studied (de la Loza and Thompson 2017; Klingenberg and Zaklan 2000; Mezey and Houle 2005; Ray et al. 2015). During the early stages of development, the tissue undergoes an Anterior-Posterior (AP) compartmentalization (García-Bellido et al. 1973). The posterior compartment becomes the source of Hedgehog (Hh) signaling, which triggers the expression of Decapentaplegic (Dpp) in a specific pattern abutting the anterior compartment (Affolter and Basler 2007). Dpp establishes a morphogen signaling axis that plays a pivotal role in guiding disc growth along the AP axis and determining the characteristic venation pattern of the adult *Drosophila* wing (Affolter and Basler 2007; Blair 2007). The longitudinal veins 2 (L2) and 5 (L5) of the adult wing are directly determined by specific landmarks of Dpp patterning (de Celis et al. 1996), but they are not symmetrically positioned with respect the AP axis (Funakoshi et al. 2001). Furthermore, the shape of the wing is remarkably robust, but clearly asymmetric. Thus, this system offers a useful model to investigate how asymmetries

arise and are robustly estab in developmentlishedal patterning. The first evidence on the origin of these asymmetries was hinted by the asymmetric pattern of phosphorylated Mad (pMad) which likely arise due to the asymmetric expression of the Dpp receptor, Thickveins (Tkv) (Funakoshi et al. 2001; Tabata and Takei 2004). However, a work by Matsuda *et al.,* (2021) has shown that while anterior patterning and growth require Dpp diffusion, it is dispensable in the posterior compartment (Akiyama and Gibson 2015; Matsuda et al. 2021).

In contrast to the AP axis, signaling along the Dorsal-Ventral (DV) axis must be symmetrical with respect to the DV boundary to ensure that the dorsal and ventral layers of the adult wing are properly formed (Liu et al. 2000). Gene expression patterns orchestrated by the AP and DV signaling axes are also instrumental for initiating planar polarization and inducing oriented proliferation, which collectively generate global forces influencing tissue morphology (Mao et al. 2011, 2013). Global forces are implicated in various morphological features, such as the formation of folds surrounding the pouch (Sui et al. 2012; Tozluoğlu et al. 2019) and the bending of the pouch at the beginning of the metamorphosis (Sui et al. 2012). While the eversion process is guided by oriented cell division and cell intercalation (de la Loza and Thompson 2017; Ray et al. 2015), the prevailing assumption is that the final wing shape primarily arises from the anchoring of wing edge cells to the cuticle, followed by retraction of the hinge (de la Loza and Thompson 2017; Dye et al. 2017; Ray et al. 2015). However, the intricate relationship between larval developmental processes and the final adult wing shape remains unclear.

AP and DV signaling are integrated by the controlled expression of the wing selector gene *vestigial (vg)* which directly depend on Dpp and Wingless (Wg) signaling (Parker and Struhl 2020; Zecca and Struhl 2007, 2021), but also on a process known as cell recruitment, which relies on contact signals between neighboring cells mediated by the protocadherins Fat and Dachsous (Zecca and Struhl 2007, 2010). In 2020, Muñoz-Nava *et al.,* studied the contribution of cell recruitment to normal wing size and showed that when it is genetically impaired, adult wings are 21% smaller than controls (Munoz-Nava et al. 2020). Interestingly, recruitment-deficient wings are also noticeably more symmetric, but this has not been studied further.

Here, we investigate the hypothesis of cell recruitment contributes to AP asymmetries in the *Drosophila* wing disc. Using morphometrics methods (Gower 1975; Krzanowski 2000) we show that lack of recruitment does result in a more symmetric wing, especially due to a reduction of the L5-M area. Contrary to expectations, this reduction of the L5-M domain is not evident during larval stages. However, lack of cell recruitment does generates a change in the shape of the *vg* pattern, transforming it into a more circular pattern. Thus, our work suggests cell recruitment may be contribute in establishing AP asymmetries in this system.

2. Materials and Methods

2.1. Fly Stocks and Crosses

All fly crosses were conducted at 25 °C. To genetically block cell recruitment we crossed (ds-Gal4, UAS-GFP;MKRS)/(SM5;TM6B, Tb) males with yw; UAS-*vg*RNAi; *vg*QELacZ/TM6B females and selected animals of the phenotype dsGal4, UASGFP/ UAS-*vg*RNAi ; MKRS/*vg*QELacZ. As a control, experiment we crossed y,w males vs yw; UAS-*vg*RNAi; *vg*QELacZ/TM6B female to obtain UAS-*vg*RNAi/+; *vg*QELacZ/+ . For the food-restricted experiment, we used animals of the control cross and restricted their food intake by reducing 90 % the amount of food.

2.2. Wing Imaginal Disc Dissection and Immunostaining

Imaginal wing discs were dissected from third-instar larvae of either sex in PEM buffer under a stereoscopic microscope. Discs were fixed in PEM-T (PEM with 0.1% of Triton X-100) with 4% paraformaldehyde for 35 minutes, washed 3 times and blocked in PEM-T with 0.5% of Bovine Serum Albumin for 2 h at room temperature. Then, samples were stained with primary antibodies at 4 °C overnight at the following dilutions: monoclonal mouse anti-DSRF a gift from S. Blair (1:250) and rabbit *β*-Galactosidase (MP Biomedicals, Cat. 55976, 1:250). Primary antibodies were detected with

Alexa Fluor 488 anti-mouse and anti-rabbit Alexa Fluor 647 (1:1000). Imaging was conducted in a Leica TC5 SP8 confocal microscope using a 40X oil-immersion objective.

2.3. Analysis of Fluorescence Patterns in Wing Disc

Z-stacks of confocal images were loaded in Python using readlif library (Negretti 2021). For analysis of *vg*QELacZ patterns, we took the Z-projection and deleted noise using the morphology function of Scikit-image. We binarized the images using the threshold function of OpenCV at 20% of the maximum pixel value in the pattern. To obtain the pre-veins pattern in the wing disc, we took the Z-projection of the DSRF staining and obtained an inverse binarization of this image using the threshold function of OpenCV. Then, we manually clicked points between DSRF intervein pattern, in order to determine vein pattern, and saved the xy coordinates in an numpy array. To measure the area of the intervein sections, we manually clicked points around the DSRF pattern to define polygons, overlaped polygons with the binarized pattern of *vg*QELacZ and measured the area within the polygons using the function contourArea of OpenCV. To measure the eccentricity of the Vg pattern we take the binarized vgQELAcZ pattern, smooth the edges using OpenCv's blur function, and compute the convex envelope of the pattern using the ConvexHull function of Python's scipy.spatial library.

2.4. Wing Mounting and Wing Areas Quantification

We sorted adult flies by sex and then dehydrated overnight in 70% ethanol. Wings were dissected in 50% ethanol and mounted in a glass coverslip. Imaging of adult wings was done using a Nikon bright-field microscope using a 4X objective. Adult wing areas were quantified using the polygon selection tool of ImageJ. We determined the border between wing blade and hinge through a straight line from the proximal border of costa to the proximal border of alula.

2.5. Procrustes Analysis

Images of adult wings were loaded in Python using the OpenCV library. We used scipy.procrustes library for Procrustes analysis. The margin landmarks (ML) consists of 10 points, 6 of which are common in prior *Drosophila* wing Procrustes analysis (Breuker et al. 2006; Klingenberg and Zaklan 2000). The other 4 points are obtained by extending the lines defined by the anterior and posterior cross veins and finding the intersection of these lines with the wing margin. The vein landmarks (VL) consists of 10 points located over the venation pattern, as in prior studies (Breuker et al. 2006; Klingenberg and Zaklan 2000).

For the symmetrization analysis of Figure 2, we obtained the midpoint between points 2A and 2P (Figure 2A) and the midpoint between points 5A and 5P. The AP axis is hereby defined as the line through these two mid points. The landmarks to quantify symmetrization consists of 10 points common in the prior *Drosophila* wing Procrustes analyses (Breuker et al. 2006; Klingenberg and Zaklan 2000), such that they can be symmetrized with respect to the AP axis defined above. Relative to this axis, vein L2 was considered symmetrical equivalent to vein L5, and vein L3 symmetrical equivalent to vein L4. To obtain the anteriorized wing, points 1A-5A were reflected with respect to the AP axis. To carry out the reflection, the straight line orthogonal to the AP axis that passed through each point of interest (1A-5A) was obtained. The distance from the line to the point was measured, and on the orthogonal line, in the posterior region, at the same distance as the point of interest, the symmetrical point was marked. For the posteriorized wing, an equivalent process was carried out, reflecting points 1P-5P with respect to the AP axis. These analysis were performed in a homemade Python code (see Supplementary Materials).

3. Results

3.1. The Inhibition of Cell Recruitment Mainly Affects the L5-M Region and Wing Shape

Previous work suggests that inhibition of cell recruitment in the *Drosophila* wing disc results in more symmetric wings (Munoz-Nava et al. 2020), but this has not been quantitatively evaluated. Thus,

we repeated the same experiment and measured relative area (*i. e.,* with respect to the total wing area) of each intervein region of the adult wing (Figure 1A,B). Strikingly, most of these regions (L1-L2, L2-L3, L3-L4) marginally increased their relative size in recruitment-impaired wings with respect to controls (Figure 1C). In contrast, the L5-M region decreased its relative size in 15% approximately (Figure 1C). Thus, unlike the result from Munoz-Nava et al. (2020) which reported that size reduction in recruitment impaired wings (relative to controls) is proportional along AP and proximal-distal axes (Munoz-Nava et al. 2020), we found that intervein areas are modified by cell recruitment asymmetrically. This effect does not depend of sex, since a similar result is obtained for male and female individuals (Figure S1A). In order to investigate if this result truly reflects a specific change in symmetries, we compared wings from flies that grew under reduced food intake, and where size is known to be systemically reduced (Parker and Struhl 2015). The wings of these flies were 25% smaller, relative to wings of normally-fed, but the relative size of each section remained unchanged (Figure S2A) suggesting that cell recruitment asymmetrically contributes to growth of the L5-M region.
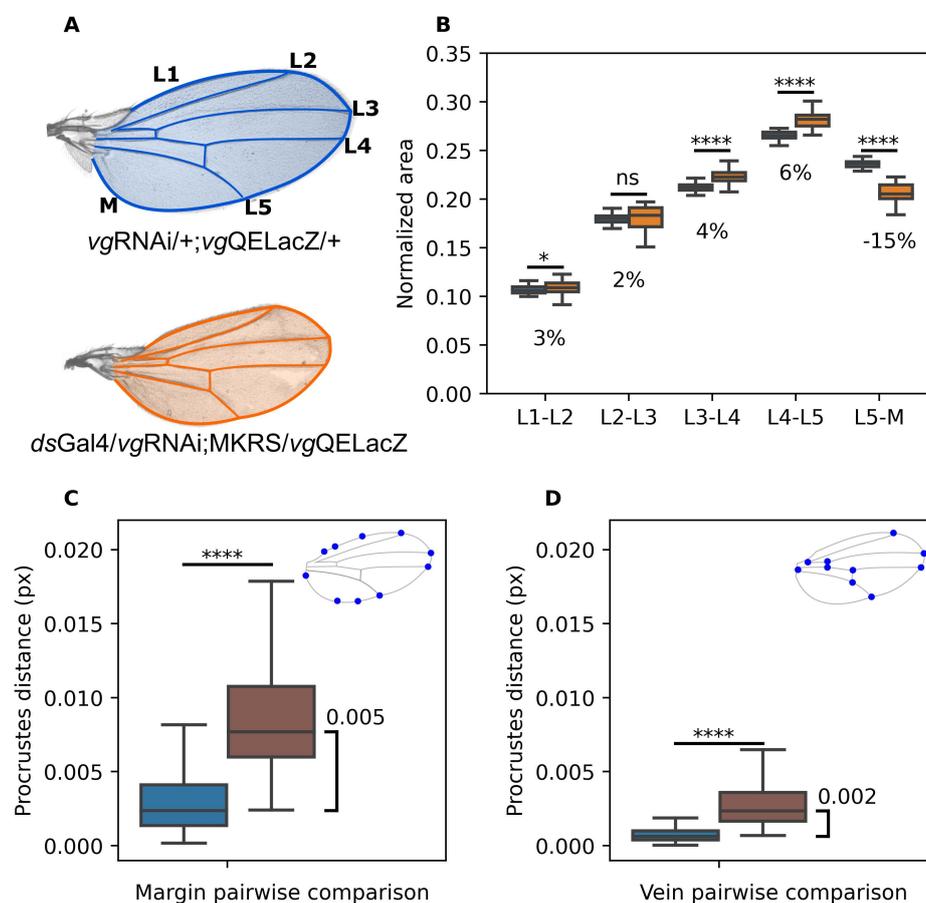

Figure 1. Blocking of cell recruitment affects mainly the area of the region L5-M and wing shape. **A.** Above, Control (male) wing showing the veins (L1-L5) and the Margin (M). In blue shading we show the wing blade, while blue lines highlight the vein pattern. Below, a representative wing from recruitment-impaired male (orange). **B**. Normalized area of each intervein region with respect to the total area of the wing. Color-coding is as in A. Numbers under the boxplot representing the percentage of reduction of medians between the groups. **C-D.** Procrustes comparison of the Margin landmarks (C) and Vein landmarks (D). Blue: Control vs. Control. Brown: Control vs. Recruitment Impaired. In the upper left corner of both plots we show representative images of ML (C) and VL (D) in representative wings. Sample sizes: Control wings (n = 52); Recruitment-impaired wings (n = 20). For the analysis using female wings see Figure S1A-C. A Shapiro test shows that distributions are non-parametric. Thus, A Mann-Whitney U test was conducted. * indicates $p < 0.05$ and **** indicates $p < 0.00005$.

In order to quantitatively measure wing shape, we used Procrustes analysis, a metric of shape changes which is scale, rotation and translation invariant (Gower 1975; Krzanowski 2000) using two different sets of landmarks defined on the wing. The first, hereby referred as the Margin Landmarks (ML, Figure 1D), are comprised of points on the wing margin of the wing and reflect overall wing shape. The second, hereby referred as the Vein Landmarks (VL, Figure 1E), are comprised of points on the wing veins and reflect the venation pattern of the wing. We compared how close recruitment-impaired wings are from control wings both using ML and VL using the Procrustes distance. As an internal comparison, we computed Procrustes distance between each pair of control wings (blue bars in Figure 1C,D) and between each pair of control vs. recruitment-impaired wings (brown bars in Figure 1C,D). We found significant difference in Procrustes distance in the control vs. recruitment-impaired comparison with respect to the control vs. control comparison, both using ML (Figure 1C) and VL (Figure 1D), but the difference in Procrustes distance is 2.5 times larger in the ML than in the VL comparison (Figure 1C,D). We conclude that lack of recruitment remarkably change wing shape while a much milder effect occurs at the venation pattern.

### 3.2. Impaired-Recruitment Wings Are More Symmetric along the AP Axis Compared to Controls

Our previous results shows that cell recruitment appears to contribute more to growth of the posterior region of the wing (particularly, the L5-M area). We then asked if cell recruitment is indeed a mechanism that contributes to AP symmetry-breaking in the *Drosophila* wing. Namely, we hypothesize that recruitment-impaired wings are more symmetric than control wings. To test this, we compared control and recruitment-impaired wings to 'symmetrized' versions of themselves. In particular, we define the Anteriorized image of a particular wing (Figure 2A) as the mirror-image reflection of the anterior part of the wing with respect to the AP axis (see Methods for a precise definition of AP axis). Conversely, the Posterior image of a particular wing is similarly defined (Figure 2A). Thus, for every wing we can measure its AP symmetry by computing the Procrustes distance to the Anteriorized and Posteriorized images of itself (Figure 2A). We found that recruitment-impaired wings are closer generally (in Procrustes distance) to both, their Anteriorized and Posteriorized images, compared to control wings. This result is even more evident when a more comprehensive set of landmarks is used (see Figure S3). We conclude that recruitment-impaired wings exhibit more AP symmetry than controls.
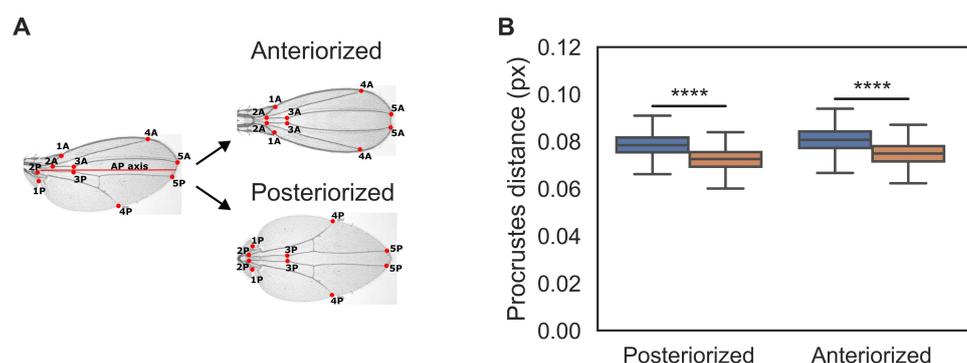
Figure 2. Recruitment-impaired wings are more symmetric compared to controls. A. Representative control wing to exemplify the process of obtaining its Anteriorized and Posteriorized image. We identified a set of 10 vein landmarks and labeled them such that for each landmark in the Anterior (A) side, there is another landmark in the posterior (P) side. This defines 5 pairs of landmarks in each wing (left). Hypothetical wings constructed in this way are mirror-image duplications of their anterior (top) and posterior (bottom) parts with respect to AP axis. **B.** Procrustes comparison for Anteriorized and Posteriorized control (blue) and recruitment-impaired wings (orange). Sample size for each set is as in Figure 1. An equivalent analysis of wings from female flies is shown in Figure S1D. A Shapiro test shows that distributions are non-parametric. Thus, a Mann-Whitney U test was conducted. **** indicates $p < 0.00005$.

3.3. Impairment of Cell Recruitment Affect the Circularity of the Wing Pouch But Does Not Affect the L5-M Intervein Area of the Drosophila Wing Disc

An interpretation of our previous results is that cell recruitment contributes to breaking the AP asymmetry of the Drosophila wing by recruiting more cells in the domain that will give rise to the L5-M region of the adult wing. But to test this we need to examine the consequences of impairing recruitment in larval stages of wing growth. Then, we analyzed a reporter of *vg*QE (vgQELacZ) in the third instar of the *Drosophila* wing disc (Figure 3A'). We co-stained these discs with antibody of DSRF (Figure 3A), a specific marker for the intervein regions (Blair, 2007), in order to measure the relative area of each intervein region. Contrary to our expectations, we did not find significant differences between the relative areas of intervein regions in controls and recruitment-impaired discs (Figure 3C).
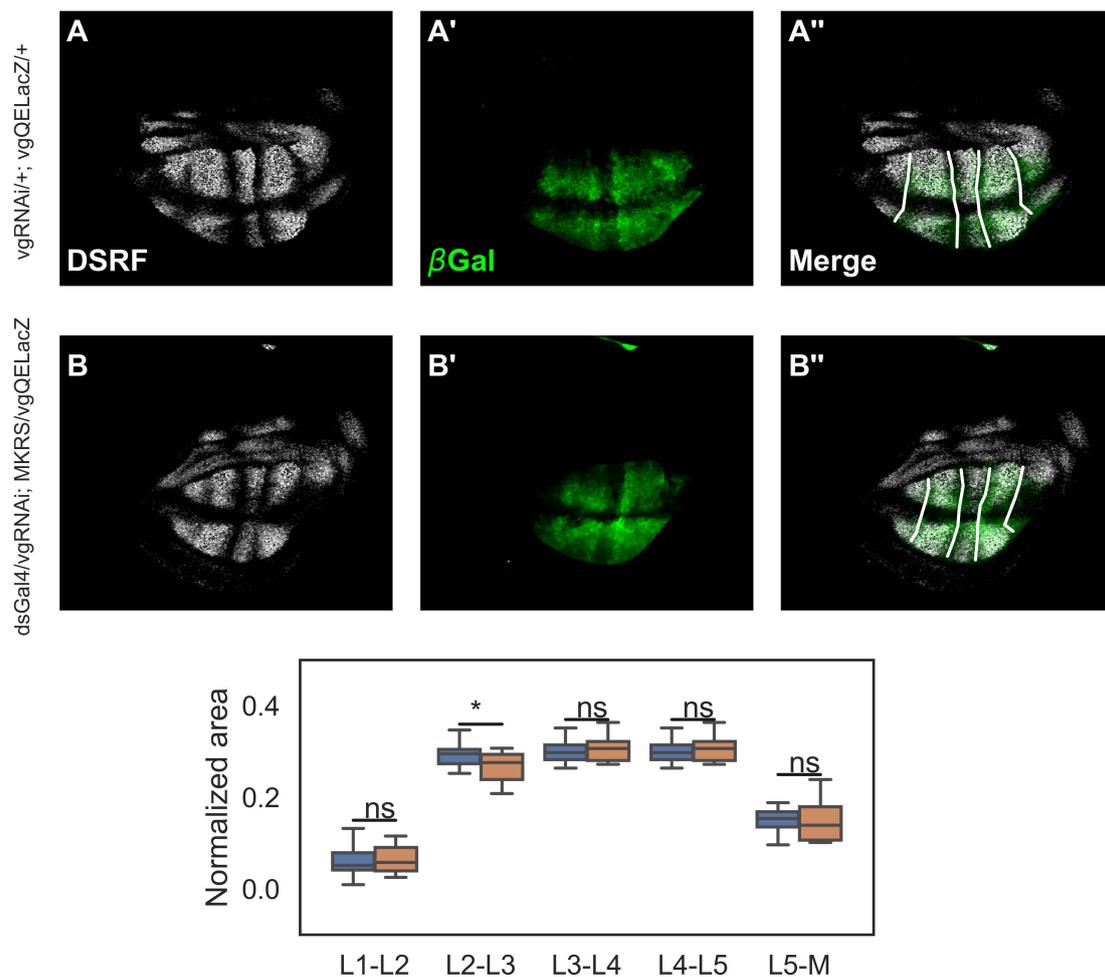
Figure 3. The reduction of the L5-M region in recruitment-impaired adult wings can not recapitulated in larval stages. A-B' Representative control (A, A') and recruitment-impaired third-instar wing discs (B, B') immunostained with DSRF (A, B, white) and β-galactosidase (A', B', green) antibodies. A'' and B'' show the merge of these patterns. All discs carry the *vg*QELacZ reporter. **C.** Normalized area with respect to the total area of the *vg*QELacZ pattern of each intervein region (see Methods). Sample sizes: Control wings (n = 36); Recruitment-impaired wings (n = 16). A Shapiro test shows that distributions are non-parametric. Thus, a Mann-Whitney U test was conducted. * indicates that $p < 0.05$.

We also examined if blocking cell recruitment has an effect on the overall shape of the wing pouch. To check this, we fitted an ellipse which passes through the contour of the *vg*QELacZ pattern (see Methods). We then measured the eccentricity of the fitted ellipses, and found that in recruitment-impaired discs, the wing pouch is more circular compared to control (*i.e.,* the eccentricity is smaller in

these patterns, Figure 4B). Taken together, our data and analysis suggest that cell recruitment does contribute to the overall shape of the the wing pouch but cannot explain why the L5-M region is smaller in adult wings.
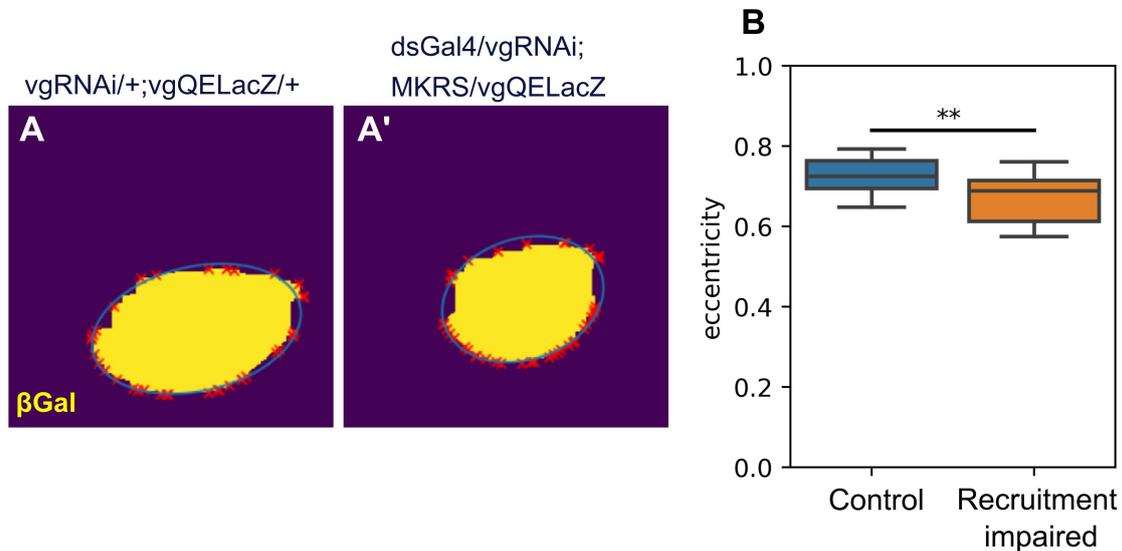
Figure 4. The pattern of *vg*QELacZ in recruitment impaired disc are more circular than controls. A-A´. Representative Control (A) and recruitment impaired (A') *vg*QELacZ binarized patterns. The representative disc used are the same as in Figure 3A', B'. **B**. Eccetricity of ellipse fitted to the *vg*QELacZ pattern using a convex envelope analysis of the pattern (see Methods). Sample size for each set is as in Figure 3. A Shapiro test shows that distributions are non-parametric. Thus, a Mann-Whitney U test was conducted. ** indicates $p < 0.01$.

4. Discussion

The developmental mechanisms underlying organ shape have been of fundamental interest in biology since the publication of D'Arcy Thompson's seminal work 'On Growth and Form' more than 100 years ago (Thompson 1917). This gave rise to the field of morphometrics, the quantitative analysis of shapes, which has advanced several disciplines, from the integration of ecology, evolution and development (eco-evo-devo) to human evolution (Klingenberg 2016; Klingenberg et al. 2004; Mitteroecker et al. 2004; Monteiro 1999; Oxnard 1978; Rohlf 1990). However, the processes orchestrating the establishment of an organ's final form remain elusive. In the search for developmental effectors underlying tissue shape, previous research has predominantly focused on examining both local and global forces acting on tissues (de la Loza and Thompson 2017; Ray et al. 2015). On the other hand, signaling pathways influencing early development have been linked to the positional information that confers identity to organs or segments (Lander et al. 2002; Wolpert 1971). In addition, the attainment of the final tissue shapes has been associated with cell movement and adherence to the extracellular matrix (Ray et al. 2015). Despite these efforts, significant gaps persist in integrating early signaling, growth, cell adhesion, and mechanical processes underlying the developmental basis of organ shape. One particular aspect that remains poorly understood in this broad problem is uncovering the origins of shape asymmetries.

The *Drosophila* wing serves as an excellent model for studying the genetics basis of organ growth and shape (Tripathi et al. 2022). Early studies in the *Drosophila* wing disc have revealed the role of *engrailed/invictus* and *apterous* in establishing the distinction of AP and DV compartments, respectively (Blair 2003; Diaz-Benjumea and Cohen 1993; Tabata et al. 1995). Strikingly, while DV patterning in the developing requires to be symmetric in order to ensure that dorsal and ventral sides of the wings match, AP patterning is inherently asymmetric, as revealed by clear differences in the positions of veins and the differences in intervein areas (Figure 1). The obvious suspect of the AP asymmetries in

the *Drosophila* wing is Dpp signaling which is indeed asymmetric due to receptor activity, leading to asymmetric pMad expression (Teleman and Cohen 2000). Yet, this asymmetry does not explain why the L1-L2 and L5-M intervein areas are remarkably different. Moreover Matsuda *et al.*, has revealed that the range of the AP signal is confined to the territory comprised between L2 and L5 (Matsuda et al. 2021). Therefore, it is unlikely that Dpp signaling could explain the asymmetry of these intervein areas (Matsuda et al. 2021). Here, we inhibited the process of cell recruitment, a mechanism that drive the expansion of *vg* through the activation of the QE. Our findings indicate that in recruitment-impaired wings, L5-M intervein area is significantly reduced (Figure 1B). Note however, that this reduction is not comparable to the relative size of the L1-L2 intervein area (Figure 1B), suggesting that while cell recruitment could contribute to this asymmetry, it cannot fully explain it and suggesting that other mechanisms act redundantly to establish AP asymmetries in the wing.

In light of the work of Matsuda et al. (2021), where it has been shown that the range of the Dpp signal is not required for the growth of the compartment beyond L5, we were surprised to find that inhibition of recruitment did not result in a significant reduction of the L5-M domain. However, we noted that while the adult wing margin has a clear border, there is not such a clear-cut end of the *vg*QE pattern in the lateral regions of the disc. Furthermore, the pattern that determines the intervein domains, marked by DSRF, overlaps exactly in the territories within veins L2-L5, but differs in lateral regions, suggesting that *vg*QE and DSRF expression could establish different territories at the edges of the pouch. Indeed, *vg* expression possibly contribute to the establishment of the wing appendages, called costa and alula (Barrio and Milán 2020), so to draw a clear boundary between the blade and these structures may not be that clear.

Another aspect that deserves some discussion is the potential role of cell recruitment in tissue mechanics. Since the wing disc is a pseudo-stratified tissue (Liu et al. 2000), the tensions generated by cell-cell anchoring depend largely on the number of cells that make up the tissue (Tozluoğlu et al. 2019). Therefore, reducing the number of cells in a specific domain of the wing disc can generate a regression of the entire tissue, in the opposite direction. Thus, the change in the circularity of the *vg*QE pattern, upon impairment of cell recruitment, could be an indirect consequence of the reduction of the number of cell beyond L5.

Our work reveals for the first time that cell recruitment in the *Drosophila* wing could have an impact on the overall asymmetric shape of adult wings. Therefore, in addition to its previously characterized role in patterning and growth, cell recruitment may also contribute to establishing asymmetric shape changes during development.

References

Affolter, Markus and Konrad Basler. 2007. The decapentaplegic morphogen gradient: from pattern formation to growth regulation. *Nature Reviews Genetics 8*(9), 663–674.

Akiyama, Takuya and Matthew C Gibson. 2015. Decapentaplegic and growth control in the developing drosophila wing. *Nature 527*(7578), 375–378.

Baker, Kari, Nathalia G Holtzman, and Rebecca D Burdine. 2008. Direct and indirect roles for nodal signaling in two axis conversions during asymmetric morphogenesis of the zebrafish heart. *Proceedings of the National Academy of Sciences 105*(37), 13924–13929.

Barrio, Lara and Marco Milán. 2020. Regulation of anisotropic tissue growth by two orthogonal signaling centers. *Developmental cell 52*(5), 659–672.

Bessodes, Nathalie, Emmanuel Haillot, Véronique Duboc, Eric Röttinger, François Lahaye, and Thierry Lepage. 2012. Reciprocal signaling between the ectoderm and a mesendodermal left-right organizer directs left-right determination in the sea urchin embryo. *PLoS Genetics 8*(12), e1003121.

Blair, Seth S. 2003. Lineage compartments in drosophila. *Current Biology 13*(14), R548–R551.

Blair, Seth S. 2007. Wing vein patterning in drosophila and the analysis of intercellular signaling. *Annu. Rev. Cell Dev. Biol. 23*, 293–319.

Breuker, Casper J, James S Patterson, and Christian Peter Klingenberg. 2006. A single basis for developmental buffering of drosophila wing shape. *PLoS one 1*(1), e7.

de Celis, Jose F, Rosa Barrio, and Fotis C Kafatos. 1996. A gene complex acting downstream of dpp in drosophila wing morphogenesis. *Nature 381*(6581), 421–424.

de la Loza, MC Diaz and BJ Thompson. 2017. Forces shaping the drosophila wing. *Mechanisms of Development 144*, 23–32.

Diaz-Benjumea, Fernando J and Stephen M Cohen. 1993. Interaction between dorsal and ventral cells in the imaginal disc directs wing development in drosophila. *Cell 75*(4), 741–752.

Dye, Natalie A, Marko Popović, Stephanie Spannl, Raphaël Etournay, Dagmar Kainmüller, Suhrid Ghosh, Eugene W Myers, Frank Jülicher, and Suzanne Eaton. 2017. Cell dynamics underlying oriented growth of the drosophila wing imaginal disc. *Development 144*(23), 4406–4421.

Ferreira, Rita R and Julien Vermot. 2017. The balancing roles of mechanical forces during left-right patterning and asymmetric morphogenesis. *Mechanisms of development 144*, 71–80.

Funakoshi, Yoko, Maki Minami, and Tetsuya Tabata. 2001. mtv shapes the activity gradient of the dpp morphogen through regulation of thickveins. *Development 128*(1), 67–74.

García-Bellido, Antonio, Pedro Ripoll, and Ginés Morata. 1973. Developmental compartmentalisation of the wing disk of drosophila. *Nature new biology 245*(147), 251–253.

Gormley, Joseph P and Nanette M Nascone-Yoder. 2003. Left and right contributions to the xenopus heart: implications for asymmetric morphogenesis. *Development genes and evolution 213*, 390–398.

Gower, John C. 1975. Generalized procrustes analysis. *Psychometrika 40*, 33–51.

Grimes, Daniel T and Rebecca D Burdine. 2017. Left–right patterning: breaking symmetry to asymmetric morphogenesis. *Trends in Genetics 33*(9), 616–628.

Klingenberg, Christian Peter. 2016. Size, shape, and form: concepts of allometry in geometric morphometrics. *Development genes and evolution 226*(3), 113–137.

Klingenberg, Christian Peter, Larry J Leamy, and James M Cheverud. 2004. Integration and modularity of quantitative trait locus effects on geometric shape in the mouse mandible. *Genetics 166*(4), 1909–1921.

Klingenberg, Christian Peter and Stefanie D Zaklan. 2000. Morphological integration between developmental compartments in the drosophila wing. *Evolution 54*(4), 1273–1285.

Krzanowski, Wojtek J. 2000. *Principles of multivariate analysis*. Oxford University Press.

Lander, Arthur D, Qing Nie, and Frederic YM Wan. 2002. Do morphogen gradients arise by diffusion? *Developmental cell 2*(6), 785–796.

Le Garrec, Jean-François, Jorge N Domínguez, Audrey Desgrange, Kenzo D Ivanovitch, Etienne Raphael, J Andrew Bangham, Miguel Torres, Enrico Coen, Timothy J Mohun, and Sigolene M Meilhac. 2017. A predictive model of asymmetric morphogenesis from 3d reconstructions of mouse heart looping dynamics. *Elife 6*, e28951.

Little, Rosie B and Dominic P Norris. 2021. Right, left and cilia: How asymmetry is established. In *Seminars in Cell & Developmental Biology*, Volume 110, pp. 11–18. Elsevier.

Liu, Xiaofeng, Muriel Grammont, and Kenneth D Irvine. 2000. Roles for scalloped and vestigial in regulating cell affinity and interactions between the wing blade and the wing hinge. *Developmental biology 228*(2), 287–303.

Mao, Yanlan, Alexander L Tournier, Paul A Bates, Jonathan E Gale, Nicolas Tapon, and Barry J Thompson. 2011. Planar polarization of the atypical myosin dachs orients cell divisions in drosophila. *Genes & development* 25(2), 131.

Mao, Yanlan, Alexander L Tournier, Andreas Hoppe, Lennart Kester, Barry J Thompson, and Nicolas Tapon. 2013. Differential proliferation rates generate patterns of mechanical tension that orient tissue growth. *The EMBO journal* 32(21), 2790–2803.

Matsuda, Shinya, Jonas V Schaefer, Yusuke Mii, Yutaro Hori, Dimitri Bieli, Masanori Taira, Andreas Plückthun, and Markus Affolter. 2021. Asymmetric requirement of dpp/bmp morphogen dispersal in the drosophila wing disc. *Nature Communications* 12(1), 6435.

Mezey, Jason G and David Houle. 2005. The dimensionality of genetic variation for wing shape in drosophila melanogaster. *Evolution* 59(5), 1027–1038.

Mitteroecker, Philipp, Philipp Gunz, Markus Bernhard, Katrin Schaefer, and Fred L Bookstein. 2004. Comparison of cranial ontogenetic trajectories among great apes and humans. *Journal of human evolution* 46(6), 679–698.

Monteiro, Leandro R. 1999. Multivariate regression models and geometric morphometrics: the search for causal factors in the analysis of shape. *Systematic Biology* 48(1), 192–199.

Munoz-Nava, Luis Manuel, Hugo Ariel Alvarez, Marycruz Flores-Flores, Osvaldo Chara, and Marcos Nahmad. 2020. A dynamic cell recruitment process drives growth of the drosophila wing by overscaling the vestigial expression pattern. *Developmental biology* 462(2), 141–151.

Negretti, Nick. 2021. readlif: Fast leica lif file reader written in python. https://github.com/nimne/readlif.

Oxnard, Charles E. 1978. One biologist's view of morphometrics. *Annual Review of Ecology and Systematics* 9(1), 219–241.

Parker, Joseph and Gary Struhl. 2015. Scaling the drosophila wing: Tor-dependent target gene access by the hippo pathway transducer yorkie. *PLoS biology* 13(10), e1002274.

Parker, Joseph and Gary Struhl. 2020. Control of drosophila wing size by morphogen range and hormonal gating. *Proceedings of the National Academy of Sciences* 117(50), 31935–31944.

Ray, Robert P, Alexis Matamoro-Vidal, Paulo S Ribeiro, Nic Tapon, David Houle, Barry J Thompson, et al. 2015. Patterned anchorage to the apical extracellular matrix defines tissue shape in the developing appendages of drosophila. *Developmental cell* 34(3), 310–322.

Rohlf, F James. 1990. Morphometrics. *Annual Review of ecology and Systematics* 21(1), 299–316.

Smith, Kelly A and Veronica Uribe. 2021. Getting to the heart of left–right asymmetry: Contributions from the zebrafish model. *Journal of Cardiovascular Development and Disease* 8(6), 64.

Sui, Liyuan, Gert O Pflugfelder, and Jie Shen. 2012. The dorsocross t-box transcription factors promote tissue morphogenesis in the drosophila wing imaginal disc. *Development* 139(15), 2773–2782.

Tabata, Tetsuya, Carol Schwartz, Elizabeth Gustavson, Zehra Ali, and Thomas B Kornberg. 1995. Creating a drosophila wing de novo, the role of engrailed, and the compartment border hypothesis. *Development* 121(10), 3359–3369.

Tabata, Tetsuya and Yuki Takei. 2004. Morphogens, their identification and regulation.

Teleman, Aurelio A and Stephen M Cohen. 2000. Dpp gradient formation in the drosophila wing imaginal disc. *Cell* 103(6), 971–980.

Thompson, J Arthur. 1917. On growth and form.

Tozluoğlu, Melda, Maria Duda, Natalie J Kirkland, Ricardo Barrientos, Jemima J Burden, Jose J Munoz, and Yanlan Mao. 2019. Planar differential growth rates initiate precise fold positions in complex epithelia. *Developmental cell* 51(3), 299–312.

Tripathi, Prabhat, Arash Firouzbakht, Martin Gruebele, and Meni Wanunu. 2022. Threading single proteins through pores to compare their energy landscapes. *Proceedings of the National Academy of Sciences* 119(39), e2202779119.

Wolpert, Lewis. 1971. Positional information and pattern formation. *Current topics in developmental biology* 6, 183–224.

Zecca, Myriam and Gary Struhl. 2007. Recruitment of cells into the drosophila wing primordium by a feed-forward circuit of vestigial autoregulation.

Zecca, Myriam and Gary Struhl. 2010. A feed-forward circuit linking wingless, fat-dachsous signaling, and the
    warts-hippo pathway to drosophila wing growth. *PLoS biology 8*(6), e1000386.

Zecca, Myriam and Gary Struhl. 2021. A unified mechanism for the control of drosophila wing growth by the
    morphogens decapentaplegic and wingless. *PLoS biology 19*(3), e3001111.